Quantum Full-Duplex Communication

Fakhar Zaman, *Student Member, IEEE*, Uman Khalid, Trung Q. Duong, *Fellow, IEEE*,
Hyundong Shin, *Fellow, IEEE*, and Moe Z. Win, *Fellow, IEEE*

Abstract— **Integrating the full-duplex capability with quantum communication potentially equips emerging wireless networks with a quantum layer of security for the stringent communication efficiency and security requirements. This paper proposes two new full-duplex quantum communication protocols to exchange classical or quantum information between two remote parties simultaneously without transferring a physical particle over the quantum channel. The first protocol, called *quantum duplex coding*, enables the exchange of a classical bit using a preshared maximally entangled pair of qubits by means of counterfactual disentanglement. The second protocol, called *quantum telexchanging*, enables the exchange of an arbitrary unknown qubit without using preshared entanglement by means of counterfactual entanglement and disentanglement. We demonstrate that quantum duplex coding and quantum telexchanging can be achieved by exploiting counterfactual electron-photon interaction gates. It is shown that these tasks can be viewed as full-duplex transmission of bits and qubits via binary erasure channels and quantum erasure channels, respectively.**

Index Terms— **6G, counterfactual communication, full-duplex communication, quantum communication.**

ACRONYMS

6G	Sixth Generation.
AO	Absorptive Object.
CQZ	Chained Quantum Zeno.
D-CNOT	Distributed Controlled-NOT.
D-MQZ	Dual Modified Quantum Zeno.
H	Horizontal.
MR	Mirror.
MQZ	Modified Quantum Zeno.
OC	Optical Oscillator.
OD	Optical Delay.
PBS	Polarizing Beamsplitter.
PR	Polarization Rotator.
QAO	Quantum Absorptive object.
QZ	Quantum Zeno.
SM	Switchable Mirror.
V	Vertical.

I. INTRODUCTION

THE sixth generation (6G) communication incorporates state-of-the-art technologies to enable emerging services such as intelligent autonomous vehicular networks, smart wearable, and three-dimensional mapping and localization. These technologies include the utilization of new spectra like terahertz band for increased communication capacity, full-duplex capability for improving attainable spectral efficiency, quantum communication for unconditional security, and quantum machine learning for intelligent network management [1], [2], [3]. For instance, full-duplex capability has been integrated with several existing as well as emerging classical technologies; namely, millimeter-wave and terahertz communication, integrated sensing and communication, massive and holographic multiple-input multiple-output transmission, and dynamic spectrum sharing to enable 6G potential applications [4], [5], [6], [7], [8].

Duplex communication systems are employed to convey information between remote parties in both directions, whereas simplex communication allows sending the information in one direction only. In full-duplex and half-duplex systems, remote parties can transfer information in both directions simultaneously and non-simultaneously, respectively. Specifically, full-duplex communication systems leverage the benefits of both time and frequency resources for simultaneous uplink and downlink operations, which can enhance the attainable spectral efficiency by a factor of two. The major challenge in implementing full-duplex communication systems is self-interference due to the power difference between the transmitted and received signals. To overcome this challenge, self-interference cancellation techniques such as passive suppression and analog/digital cancellation have been proposed. However, designing efficient self-interference cancellation techniques is still a challenging task [9].

In contrast to classical communication, quantum communication enables full duplexity by quantum dialogue [10], [11], [12], [13] and quantum state exchange [14], [15], [16], [17], based on the unique properties of the quantum mechanics such as quantum entanglement [18], [19], [20]. The quantum dialogue [10], [11], [12], [13] provides a novel way of

exchanging classical information by utilizing the preshared entanglement, which is unattainable in classical communication. However, it requires multiple entangled pairs to exchange even one bit of classical information. This paper proposes a full-duplex protocol, which allows remote parties to exchange one bit of classical information by using only one entangled pair but no physical particle is transmitted over neither quantum nor classical channels. The quantum state exchange allows remote parties to exchange quantum information by means of *preshared entanglement*, local operations, and classical announcements [14], [15], [16], [17]. However, the amount of information exchanged between remote parties depends on the amount of preshared entanglement. This paper proposes a full-duplex protocol, which allows remote parties to exchange one qubit of quantum information without using preshared entanglement and without transmitting any physical particle over the quantum channel.

Counterfactual quantum communication enables remote parties to transmit information without transmitting any physical particle over the channel [21], [22], [23], [24], [25], [26]. Counterfactuality was first introduced in the context of counterfactual quantum computation [27], [28], [29], [30] followed by the counterfactual quantum cryptography [31], [32], [33], [34], [35], [36], [37]. The basic concept is originated from the interaction-free measurement to ascertain the presence or absence of an absorptive object (AO) in an interferometer without physically interrogating it [38], [39]. The counterfactual quantum communication is based on the chained quantum Zeno (CQZ) effect where the classical information is encoded as the presence or absence of an AO in the interferometer [21], [22], [40]. In contrast, transferring the quantum information requires a quantum AO which can be in the superposition of presence and absence states [41], [42], [43], [44], [45], [46].

In quantum mechanics, the hidden assumption of a pre-shared phase reference[1] between remote parties [48], [49] and the presence of the channel noise [50], [51], [52] are the bottlenecks of quantum communication and remote computation protocols. Furthermore, although quantum communication provides a novel way of secure communication under unconditional security [19], [53], [54], [55], [56], [57], [58], recently, it has been shown that counterfactual attacks pose a threat to conventional quantum cryptography protocols [59]. In counterfactual quantum communication, only local quantum operations are required as no physical particle is transmitted over the quantum channel between remote parties. Therefore, a counterfactual setup (i) allows independent local definitions of phase reference [60]; (ii) can outperform conventional quantum teleportation in the presence of severe depolarizing and bit-flip quantum noise [60]; and (iii) has the potential to provide security against counterfactual attacks [31], [59]. Due to the aforementioned advantages of the coutnerfactual quantum communication, it has gained attention in last one decade [61], [62], [63], [64], [65], [66].

This paper proposes two new full-duplex counterfactual quantum communication protocols called *quantum duplex coding* and *quantum telexchanging* to transmit classical and quantum information between two remote parties in both directions simultaneously, respectively. The protocols are accomplished by designing *nonlocal* operations by exploiting the inherent property of the counterfactual quantum communication. The key contributions of this paper are two full-duplex quantum communication protocols, which are described as follows:

- *Quantum Duplex Coding*: The protocol enables each party to transmit one bit of classical information in each direction simultaneously without transferring any physical particle over neither quantum nor classical channels. The full-duplex capability is achieved by using a single preshared Bell pair by means of counterfactual disentanglement. It is shown that the quantum duplex coding can be viewed as full-duplex transmission of bits via binary erasure channels.
- *Quantum Telexchanging:* The protocol enables each party to transmit one qubit of quantum information in each direction simultaneously without transferring any physical particle over quantum channels. The full-duplex capability is achieved without using preshared entanglement by means of counterfactual entanglement and disentanglement. It is shown that the quantum telexchanging can be viewed as full-duplex transmission of qubits via quantum erasure channels.

The remaining sections are organized as follows: Section III briefly explains the preliminaries to design quantum duplex coding and telexchanging protocols. In Section IV, the quantum duplex coding protocol is proposed by designing modified quantum Zeno (MQZ) and distributed controlled-NOT (D-CNOT) gates to transfer classical information in both directions simultaneously. In Section V, the quantum telexchanging protocol is demonstrated by designing dual MQZ (D-MQZ) and dual D-CNOT gates for quantum state exchange in a counterfactual way. Section VI briefly describes how the information is transferred in counterfactual quantum communication. Finally, Section VII gives our conclusions and final remarks.

Notations: Random variables are displayed in sans serif, upright fonts; their realizations in serif, italic fonts. Vectors and matrices are denoted by bold lowercase and uppercase letters, respectively.

II. QUANTUM INFORMATION

A. Quantum States

A classical bit or simply a bit is the basic information unit in classical information processing, which is characterized by either 0 or 1. A quantum bit or a qubit in short, is a quantum counterpart of the bit, which is a two-dimensional state vector that can be decomposed into a linear combination of orthonormal basis states—called *quantum superposition*. The orthonormal basis states $|0\rangle$ and $|1\rangle$ are commonly used in quantum information processing, called the computational basis states, which are analogous to the classical bits 0 and 1.

---

[1]The existence of common definitions of quantum superposition states and non-diagonal Hamiltonian evolution.

Generally, a quantum state is represented as a d-dimensional state vector, called a qudit, and can be decomposed into a linear combination of d-dimensional orthonormal basis states. The state of a quantum system can be a either pure or mixed state. Note that a pure quantum state is a linear combination of basis states, whereas a mixed state is a convex combination of multiple pure states of same dimension.

B. Quantum Entanglement

We have seen that a single bit has two possible states. The number of possible states increases exponentially with the number of bits. For example, a 2-bit classical system has four possible states $00, 01, 10$, and 11. Similarly, a two-qubit quantum system can be in superposition of four orthonormal basis states. In addition to pure and mixed states, multi-qubit quantum states can be further categorized as separable states (independent to each other) and entangled states (quantum-correlated to each other). For instance, Bell states denote two-qubit maximally entangled states, which have no counterpart in the classical mechanics. The entanglement denotes the quantum correlation between multi-qubit systems, which allows to infer the measurement results of all qubits by measuring one qubit only. In quantum information science, the quantum entanglement is an important resource to: i) ensure the security of the communication network; ii) enhance the Fisher information of the unknown parameter to be estimated; and iii) increase the computation capability of the quantum computer.

C. Quantum Measurements

The measurements are performed to determine the properties of the system under observation. In a classical system, the measurements performed on a classical variable do not affect the system state. In contrast, the state of the quantum system collapses to one of the orthonormal basis states, called the post-measurement states. For example, consider that a single-qubit state $|\psi\rangle = a_0 |0\rangle + a_1 |1\rangle$ is measured in computational basis. Then, the system state collapses to $|0\rangle$ and $|1\rangle$ with probability $|a_0|^2$ and $|a_1|^2$, respectively, where $|a_0|^2 + |a_1|^2 = 1$. Therefore, the quantum measurement irreversibly transforms the original state of the quantum system. For a multi-qubit system, measurements can be performed either on the complete system or the part of the system. For a separable state, the measurement on one qubit does not affect the state of the other qubit. In contrast, the measurement on one half of the entangled system does affect the state of the other half of the system and the state becomes immediately known with certainty. This surprising phenomenon of quantum mechanics plays an important role to detect the presence of an eavesdropper in the quantum channel.

III. COUNTERFACTUAL QUANTUM COMMUNICATION

Counterfactual quantum communication is based on the single-particle nonlocality and quantum measurement theory. In general, the state of a quantum system evolves under the internal Hamiltonian of the system. A quantum state collapses
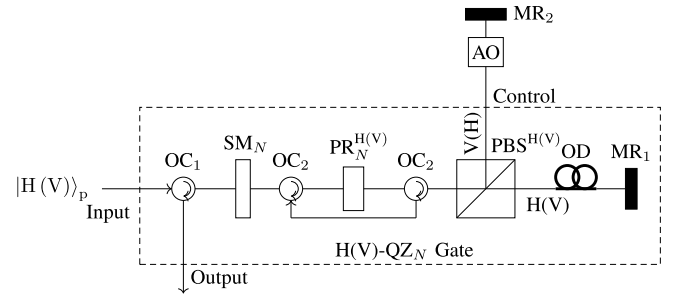

Fig. 1. A H(V)-QZ$_N$ gate with N cycles where H (V) stands for horizontal (vertical) polarization of the photon, OC for an optical circulator, SM for a switchable mirror, PR for a polarizing rotator, PBS for a polarizing beam splitter, OD for an optical delay, MR for a mirror, and AO shows the absorptive state of an object.

back to its initial state if the time between repeated measurements Δt approaches to zero—called the *quantum Zeno (QZ) effect* [67]. The QZ effect has been demonstrated to achieve interaction-free measurement—i.e., *ability to determine the presence of an object in a certain region without interacting with it*—where the state of a photon acts as an unstable quantum state corresponding to the presence of the AO [39]. This section begins by introducing a brief review of the overall actions of the QZ and CQZ gates [64], [68] that are invoked to formulate the D-CNOT and dual D-CNOT operations to transfer classical and quantum information in both directions simultaneously.

A. QZ Gates

Fig. 1 shows the Michelson version of the QZ gate [68] to perform the interaction-free measurement. The QZ gate is to ascertain the classical behavior of an AO, i.e., to infer the absence state $|0\rangle_{AO}$ or the presence state $|1\rangle_{AO}$ of AO without interacting with it. The H(V)-QZ$_N$ gate takes an H (V) polarized photon as input where H (V) denotes the horizontal (vertical) polarization of the photon. The switchable mirror SM$_N$ is initially turned off to allow the passing of the photon and is turned on for N cycles once the photon is passed. After N cycles, SM$_N$ is turned off again allowing the photon out. The polarization rotator PR$_N^{H(V)}$ gives rotation to the input photon by an angle $\theta_N = \pi/(2N)$ as follows:

$$\mathrm{PR}_N^{\mathrm{H(V)}} : \begin{cases} |\mathrm{H\,(V)}\rangle_\mathrm{p} \rightarrow \cos\theta_N |\mathrm{H\,(V)}\rangle_\mathrm{p} + \sin\theta_N |\mathrm{V\,(H)}\rangle_\mathrm{p}, \\ |\mathrm{V\,(H)}\rangle_\mathrm{p} \rightarrow \cos\theta_N |\mathrm{V\,(H)}\rangle_\mathrm{p} - \sin\theta_N |\mathrm{H\,(V)}\rangle_\mathrm{p}. \end{cases}$$
(1)

The photon state $|\phi\rangle$ after $\mathrm{PR}_N^{\mathrm{H(V)}}$ in the first cycle of the H(V)-QZ$_N$ gate is given by

$$|\phi\rangle = \cos\theta_N |\mathrm{H\,(V)}\rangle_\mathrm{p} + \sin\theta_N |\mathrm{V\,(H)}\rangle_\mathrm{p}.$$
(2)

Then, the polarizing beam splitter PBS separates the H and V components of the photon into two different optical paths: SM $\rightarrow$ MR$_1$ and SM $\rightarrow$ MR$_2$. The H (V) component goes towards MR$_1$ and the V (H) component goes towards MR$_2$. The photon component in the second optical path only interacts with the AO (control terminal).

- AO $= |0\rangle_{AO}$: In the absence of the AO, the V (H) component of the photon is reflected by MR$_2$ and is returned to

TABLE I
H(V)-QZ$_N$ AND H(V)-CQZ$_{M,N}$ GATES

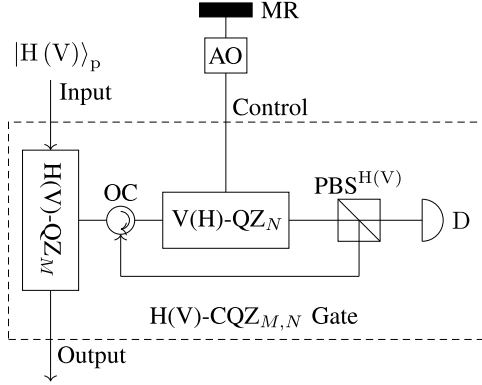| Input	Control	QZ Gate			CQZ Gate		
		Output	Probability	Counterfactuality	Output	Probability	Counterfactuality
$\lvert H\,(V)\rangle_p$	$\lvert 0\rangle_{AO}$	$\lvert V\,(H)\rangle_p$	1	No	$\lvert H\,(V)\rangle_p$	λ_0	Yes
	$\lvert 1\rangle_{AO}$	$\lvert H\,(V)\rangle_p$	μ	Yes	$\lvert V\,(H)\rangle_p$	λ_1	Yes

Fig. 2. A H(V)-CQZ$_{M,N}$ gate with M outer and N inner cycles where D is a photon detector. Table I shows the overall action of the H(V)-CQZ$_{M,N}$ gate.

PBS. Hence, the photon state remains unchanged. After $n\,(<N)$ cycles, the photon state is given by

$$|\phi\rangle = \cos\,(n\theta_N)\,\lvert H\,(V)\rangle_p + \sin\,(n\theta_N)\,\lvert V\,(H)\rangle_p. \quad (3)$$

The photon will end up in the state $\lvert V\,(H)\rangle_p$ with certainty by $\pi/2$ rotation after N cycles.

- AO $= \lvert 1\rangle_{AO}$: In the presence of the AO, the V (H) component is absorbed by the AO if it is found in the control terminal. In each cycle, the probability of this absorption event is equal to $\sin^2\theta_N$. Unless the photon is absorbed, the photon state collapses to the initial state $\lvert H\,(V)\rangle_p$. After N cycles, the photon is not absorbed and ends up in the state $\lvert H\,(V)\rangle_p$ with the probability

$$\mu = \cos^{2N}\theta_N \quad (4)$$

tending to one as $N \to \infty$.

Table I shows the overall action of the QZ gate. Note that the H(V)-QZ$_N$ gate has the output $\lvert H\,(V)\rangle_p$ in the presence state $\lvert 1\rangle_{AO}$ if the photon has not traveled over the control terminal (quantum channel). Hence, the QZ gate is counterfactual only for this measurement outcome.

B. CQZ Gates

Fig. 2 shows the nested version of QZ gates with M outer and N inner cycles [64]. The CQZ gate enables ascertaining the absence or presence of the AO counterfactually for both outcomes. The H(V)-CQZ$_{M,N}$ gate also takes an H (V) polarized photon as input. In each outer cycle, the V (H) component of the photon enters the inner V(H)-QZ$_N$ gate.

- AO $= \lvert 0\rangle_{AO}$: In the absence of the AO, the inner V(H)-QZ$_N$ gate transforms the photon state $\lvert V\,(H)\rangle_p$ into

$\lvert H\,(V)\rangle_p$ after N cycles. This component ends up at the detector D after PBS. Hence, the inner QZ gate acts as an AO for the outer QZ gate in the absence state $\lvert 0\rangle_{AO}$, where D serves to detect the event that the photon is found in the control terminal. In each outer cycle, unless the photon is discarded, the photon state collapses back to the initial state $\lvert H\,(V)\rangle_p$ with the probability $\cos^2\theta_M$, where $\theta_M = \pi/\,(2M)$. After M outer cycles, the photon is not discarded at detector D and ends up in the initial state $\lvert H\,(V)\rangle_p$ with the probability

$$\lambda_0 = \cos^{2M}\theta_M. \quad (5)$$

tending to one as $M \to \infty$.

- AO $= \lvert 1\rangle_{AO}$: In case the AO is present, the V (H) component of the photon recombines with the H (V) component and the photon state remains unchanged for the next outer cycle unless the photon is absorbed by the AO. Hence, the inner QZ gate acts as a mirror for the outer QZ gate in the presence state $\lvert 1\rangle_{AO}$. After $i\,(<M)$ outer cycles, unless the photon is absorbed, the photon state is given by $|\phi\rangle = \cos\,(m\theta_M)\,\lvert H\,(V)\rangle_p + \sin\,(m\theta_M)\,\lvert V\,(H)\rangle_p$, which is again not absorbed by the AO for the next outer cycle with the probability

$$\left[1 - \sin^2\,(i\theta_M)\sin^2\theta_N\right]^N. \quad (6)$$

Hence, unless the photon is absorbed by the AO, the H(V)-CQZ$_{M,N}$ gate transforms the input state $\lvert H\,(V)\rangle_p$ into $\lvert V\,(H)\rangle_p$ with the probability

$$\lambda_1 = \prod_{i=1}^{M}\left[1 - \sin^2\,(i\theta_M)\sin^2\theta_N\right]^N \quad (7)$$

tending to one as $M, N \to \infty$.

Note that the CQZ gate is counterfactual for both the outcomes and infers the absence or presence of the AO (with the probability λ_0 or λ_1) but no physical particle (photon) is found in the control terminal (see Table I).

C. Counterfactual Communication

A communication task can be achieved in a counterfactual way by using the QZ or CQZ gate where the sender (Alice) has an AO and the receiver (Bob) equips the (C)QZ gate [21], [22]. To transfer a classical bit $b \in \{0,1\}$, Alice encodes this information as
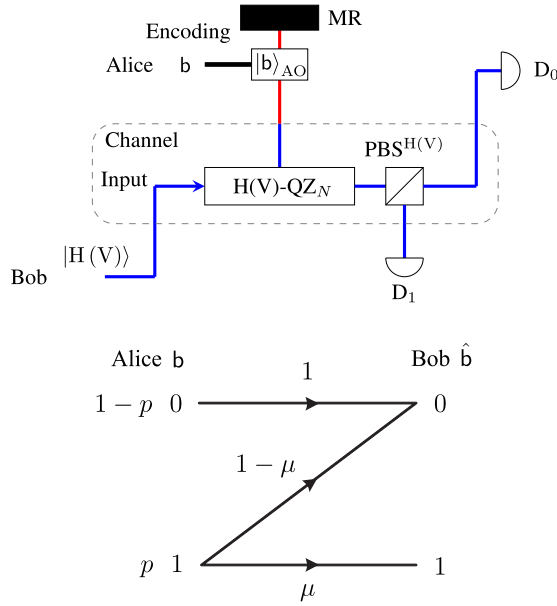
$$AO = \lvert b\rangle_{AO}. \quad (8)$$

Fig. 3. H(V)-QZ$_N$ counterfactual communication where Alice encodes her classical message b in the AO state $|b\rangle_{AO}$ and Bob throws his H (V) polarized photon towards the H(V)-QZ$_N$ gate to decode this message corresponding to the detector D$_b$ clicks. This QZ counterfactual communication forms a classical binary Z-channel with the error probability $1 - \mu$ for b = 1.
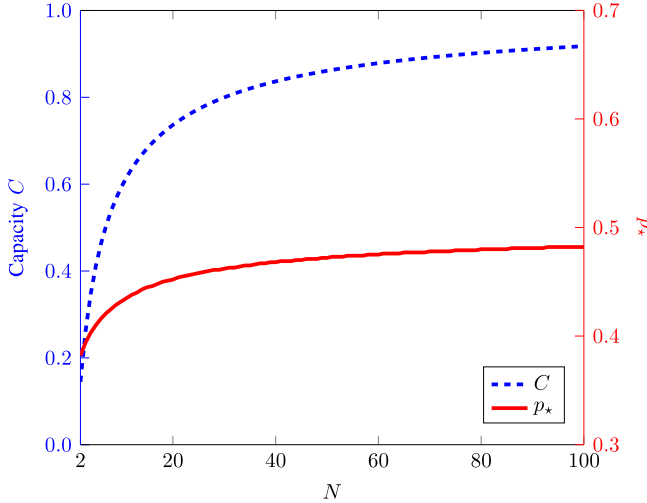

Fig. 4. Capacity C [bits/photon] and the capacity-achieving distribution $p_\star$ for the H(V)-QZ$_N$ counterfactual communication as a function of N. The 80 % efficiency ($C = 0.8$ bits/photon) is achieved at $N = 31$ with $p_\star = 0.463$.

1) QZ Simplex Communication: The communication with the QZ gate is counterfactual only for the one classical bit—i.e., *semi-counterfactual* [21], [68]. The photon is found in the transmission channel with the probability one for b = 0. Bob equips only a single-photon source and detector D$_1$ as shown in Fig. 3. The QZ gate is the part of the transmission channel where the input terminal is connected with the single-photon source [40]. Bob starts the protocol by generating his H (V) polarized single photon and inputting it to the H(V)-QZ$_N$ gate. Bob decides $\hat{b} = 1$ if D$_1$ clicks. Otherwise Bob decides $\hat{b} = 0$. Note that if the photon is discarded in the QZ gate for b = 1, Bob decodes erroneously the classical information as $\hat{b} = 0$, which forms a classical binary Z-channel [69].
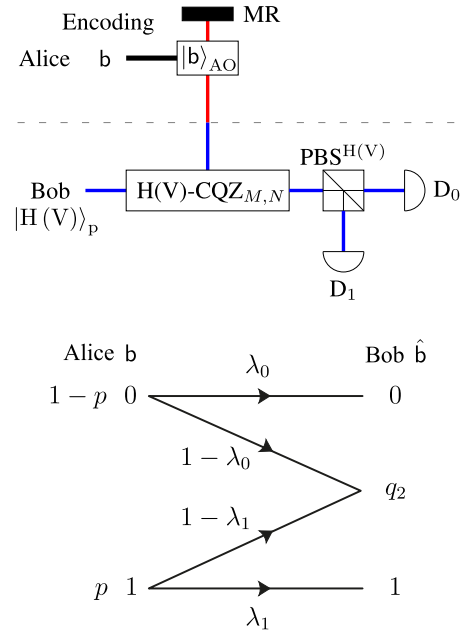

Fig. 5. H(V)-CQZ$_{M,N}$ counterfactual communication where Alice encodes her classical message b in the AO state $|b\rangle_{AO}$ and Bob throws his H (V) polarized photon towards the H(V)-CQZ$_{M,N}$ gate to decode this message corresponding to the detector D$_b$ clicks. This CQZ counterfactual communication forms a classical asymmetric binary erasure channel with the erasure probability $1 - \lambda_b$ for the message b.

Let $p = \Pr[b = 1]$. Then, the mutual information $I(A; B)$ between Alice (A) and Bob (B) is given by

$$I(A; B) = h(p) - q_1 h\left(\frac{p(1 - \mu)}{q_1}\right), \qquad (9)$$

where $h(p) = -p \log_2(p) - (1 - p) \log_2(1 - p)$ is the binary entropy function and

$$\begin{aligned} q_1 &= \Pr[\hat{b} = 0] \\ &= (1 - p) + p(1 - \mu). \end{aligned} \qquad (10)$$

By optimizing the message distribution p such that

$$\left[\partial I(A; B) / \partial p\right]\big|_{p=p_\star} = 0, \qquad (11)$$

we obtain the capacity C in bits/photon for the QZ semi-counterfactual communication as follows:

$$C = \left[I(A; B)\right]\big|_{p=p_\star}. \qquad (12)$$

Note that the capacity C for this simplex communication has the minimum value of 0.144 bits/photon with $p_\star = 0.382$ when $N = 2$ and tending to 1 bit/photon with $p_\star = 1/2$ as $N \to \infty$ (see Fig. 4).

2) CQZ Simplex Communication: To communicate both 0 and 1 without transmitting any physical particle over the transmission (quantum) channel, Bob uses the CQZ gate as shown in Fig. 5. Bob starts the protocol for decoding the information by throwing his H (V) polarized photon towards the H(V)-CQZ$_{M,N}$ gate and decides that the message 0 or 1 was transmitted if it ends up in the state $|H(V)\rangle_p$ or $|V(H)\rangle_p$. That is, the CQZ receiver decides the decoded message as b if D$_b$ clicks. Otherwise, Bob declares that the photon is erasured (discarded or absorbed).
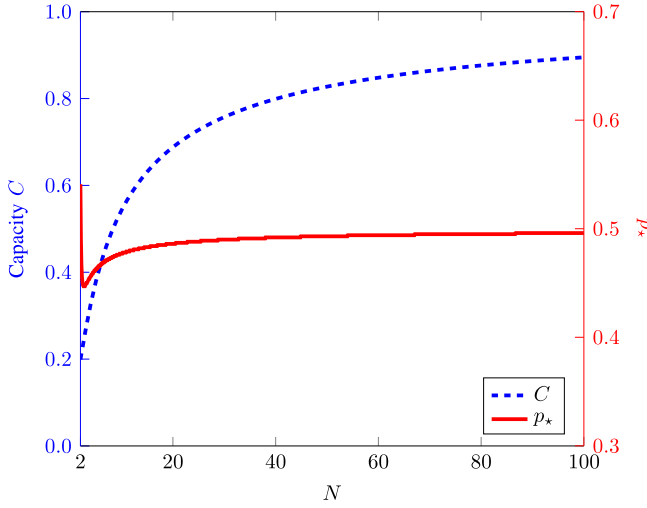
Fig. 6. Capacity C [bits/photon] and the capacity-achieving distribution $p_\star$ for the H(V)-CQZ$_{M,N}$ counterfactual communication as a function of N when $M = 2$. With the smallest outer cycles ($M = 2$), the 80% efficiency ($C = 0.8$ bits/photon) is achieved at $N = 81$ with $p_\star = 0.466$.
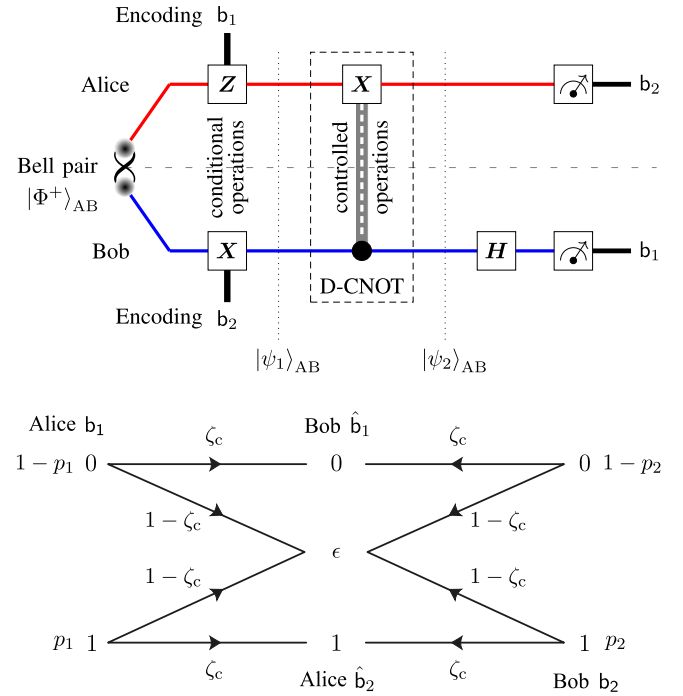

Fig. 7. Quantum duplex coding for classical information $b_1 b_2$ where $p_i = \Pr[b_i = 1]$ and $i \in \{1, 2\}$. For the D-CNOT operation, Alice's qubit acts as a target bit and Bob's qubit acts as a control bit in a counterfactual way. Here, H is the Hadamard gate and Z represents the Pauli z operator, respectively; b_1 (or b_2) is the classical bit Alice (or Bob) wants to transmit to Bob (or Alice); $|\psi_1\rangle_{\text{AB}}$ is the encoded Bell state; and $|\psi_2\rangle_{\text{AB}}$ is the disentangled state by the D-CNOT operation (viewed as counterfactual full-duplex transmission) for decoding the message. The quantum duplex coding forms a full-duplex binary erasure channel with the erasure probability $1 - \zeta_c$ for the message $b_1 b_2$.

IV. QUANTUM DUPLEX CODING

In this section, we develop a full-duplex quantum protocol to transfer classical information in both directions simultaneously and counterfactually.

A. Protocol

Consider that Alice and Bob have a preshared maximally entangled pair (Bell state):

$$\left|\Phi^+\right\rangle_{\text{AB}} = \frac{1}{\sqrt{2}} |00\rangle_{\text{AB}} + \frac{1}{\sqrt{2}} |11\rangle_{\text{AB}}, \tag{15}$$

where the subscripts A and B denote Alice and Bob, respectively. Alice and Bob encode the classical message $b_1 b_2$ in $|\psi_1\rangle_{\text{AB}}$ where b_1 is the classical bit Alice wants to send to Bob and b_2 is vice versa as follows (see Fig. 7) [68]:

$$|\psi_1\rangle_{\text{AB}} : \begin{cases} 00 \to (\boldsymbol{I} \otimes \boldsymbol{I}) \left|\Phi^+\right\rangle_{\text{AB}} = \left|\Phi^+\right\rangle_{\text{AB}}, \\ 01 \to (\boldsymbol{I} \otimes \boldsymbol{X}) \left|\Phi^+\right\rangle_{\text{AB}} = \left|\Psi^+\right\rangle_{\text{AB}}, \\ 10 \to (\boldsymbol{Z} \otimes \boldsymbol{I}) \left|\Phi^+\right\rangle_{\text{AB}} = \left|\Phi^-\right\rangle_{\text{AB}}, \\ 11 \to (\boldsymbol{Z} \otimes \boldsymbol{X}) \left|\Phi^+\right\rangle_{\text{AB}} = \left|\Psi^-\right\rangle_{\text{AB}}, \end{cases} \tag{16}$$

where $\boldsymbol{I}$ is the identity operator; $\boldsymbol{X}$ and $\boldsymbol{Z}$ represent Pauli x and z operators, respectively; and

$$\left|\Phi^\pm\right\rangle_{\text{AB}} = \frac{1}{\sqrt{2}} |00\rangle_{\text{AB}} \pm \frac{1}{\sqrt{2}} |11\rangle_{\text{AB}}, \tag{17}$$

$$\left|\Psi^\pm\right\rangle_{\text{AB}} = \frac{1}{\sqrt{2}} |01\rangle_{\text{AB}} \pm \frac{1}{\sqrt{2}} |10\rangle_{\text{AB}}. \tag{18}$$

In case the photon is found in the transmission channel, it is either discarded by the detector in the CQZ gate (when b = 0 with the probability $(1 - \lambda_0)^2$ or absorbed by the AO (when b = 1 with the probability $1 - \lambda_1$). Hence, this CQZ counterfactual communication forms a classical (but not symmetric) binary erasure channel [69] and the mutual information $I(\text{A}; \text{B})$ is given by

$$I(\text{A}; \text{B}) = h(p) - q_2 h\left(\frac{p(1 - \lambda_1)}{q_2}\right), \tag{13}$$

where

$$\begin{aligned} q_2 &= \Pr[\text{b is erasured}] \\ &= (1 - p)(1 - \lambda_0) + p(1 - \lambda_1). \end{aligned} \tag{14}$$

We calculate the capacity C in bits/photon by maximizing the mutual information with the optimal distribution $p_\star$. Note that the capacity C for this CQZ counterfactual communication has the minimum value of 0.1515 bits/photon with $p_\star = 0.606$ when $N = M = 2$ and tending to 1 bit/photon with $p_\star = 1/2$ as $M, N \to \infty$ (see Fig. 6).

Using the dual CQZ gate, the counterfactual Bell-state analysis has been proposed in [64] to achieve the distinguishability task of four Bell states without transmitting a physical particle over the transmission channel. In this dual CQZ Bell-state analyzer, one entangled particle (electron) of the Bell pair acts as a quantum AO and the other entangled particle (photon) is input to the dual CQZ gate to perform the counterfactual CNOT operation. To improve the efficiency of quantum superdense coding, the semi-counterfactual Bell-state analyzer has been also proposed in [68] using the dual QZ gate (instead of the dual CQZ gate) with the sacrifice of full counterfactuality. This dual QZ superdense coding achieves 90% efficiency (1.8 bits/qubit) when $N = 12$.

---

[2] In this case, Bob knows that b = 0 but the photon is discarded by the protocol for counterfactuality.
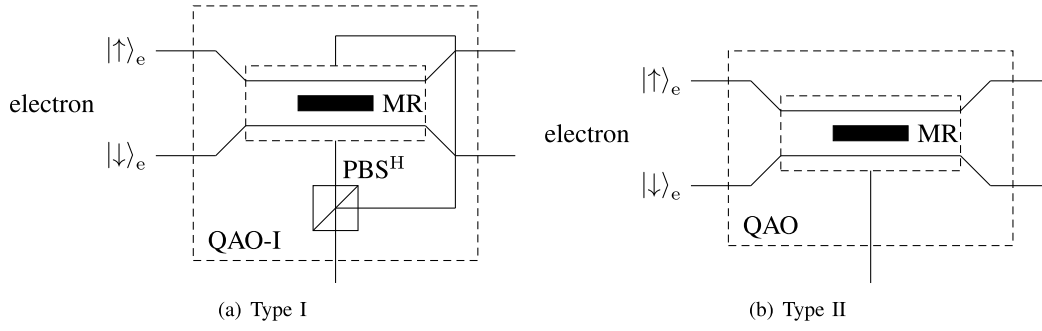
Fig. 8. A quantum AO (electron) for (a) the QZ gate (type I) and (b) the CQZ gate (type II). The electron takes the superposition of two paths $|\uparrow\rangle_e$ and $|\downarrow\rangle_e$. In type I, the electron states $|\uparrow\rangle_e$ and $|\downarrow\rangle_e$ act as the presence (absence) state $|1\,(0)\rangle_{AO}$ and the absence (presence) state $|0\,(1)\rangle_{AO}$ of the AO for the H(V)-QZ gate, respectively. In type II, the electron states simply act as $|\uparrow\rangle_e = |0\rangle_{AO}$ and $|\downarrow\rangle_e = |1\rangle_{AO}$ for the CQZ gate. If the photon is absorbed by the electron, the electron state is in an erasure state orthogonal to $|\uparrow\rangle_e$ and $|\downarrow\rangle_e$.
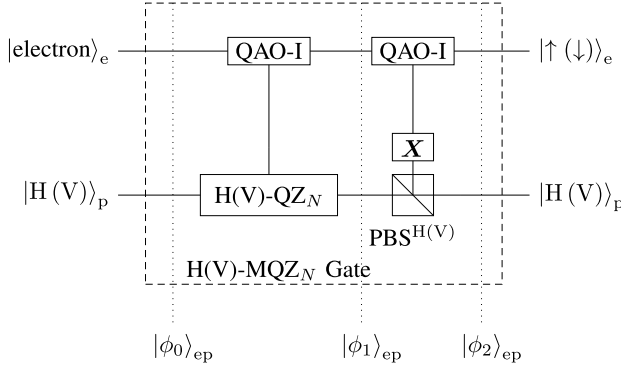

Fig. 9. A H(V)-MQZ$_N$ interaction where the superposition state $|\text{electron}\rangle_e = \alpha|\uparrow\rangle_e + \beta|\downarrow\rangle_e$ of the quantum AO (electron) is collapsed to $|\uparrow\,(\downarrow)\rangle_e$ (dequantumization) using the H(V)-QZ$_N$ gate unless the photon is absorbed by the electron. If the photon is found in the quantum channel, the pair of photon and electron is discarded in transforming $|\phi_1\rangle_{ep}$ to $|\phi_2\rangle_{ep}$ where the photon that has traveled over the channel is diverted again to the quantum AO and absorbed by the electron. This electron-photon interaction is designed to output the photon and electron by using the presence state (blocking event) only. Hence, the protocol is fully counterfactual.

The duplex encoding transforms the initial Bell state $|\Phi^+\rangle_{AB}$ to $|\psi_1\rangle_{AB}$, one of the four Bell states $|\Phi^\pm\rangle_{AB}$ and $|\Psi^\pm\rangle_{AB}$.

To transfer the classical information in both directions simultaneously, Alice and Bob perform the D-CNOT operation in a counterfactual way where Alice's qubit acts as a target bit and Bob's qubit acts as a control bit. The D-CNOT operation *disentangles* the encoded Bell state $|\psi_1\rangle_{AB}$ to produce $|\psi_2\rangle_{AB}$ as follows:

$$|\psi_2\rangle_{AB} : \begin{cases} |\Phi^\pm\rangle_{AB} & \to |0\rangle_A |\pm\rangle_B, \\ |\Psi^\pm\rangle_{AB} & \to |1\rangle_A |\pm\rangle_B, \end{cases} \quad (19)$$

where $|\pm\rangle = (|0\rangle \pm |1\rangle)/\sqrt{2}$ is the Hadamard basis. To decode the classical information, Alice directly measures her qubit and decides the one-bit message b_2, whereas Bob first applies the Hadamard gate H followed by measuring his qubit in computational basis and decodes one-bit message b_1. Alice and Bob decide the decoded messages as b_2 and b_1 from their post-measurement states $|b_2\rangle_A$ and $|b_1\rangle_B$, respectively. Here it is important to note that whenever a physical particle is found in the quantum channel during the implementation of the D-CNOT operation, the protocol discards it and declares an erasure of the classical information $b_1 b_2$.

TABLE II
DECODING THE CLASSICAL MESSAGE $b_1 b_2$ FOR THE
MQZ DUPLEX CODING

Alice		Bob	
Electron	b_2	Photon	b_1
$|\uparrow\rangle_e$	0	$|H\rangle_p$	0
$|\downarrow\rangle_e$	1	$|V\rangle_p$	1

B. MQZ Duplex Coding

In this section, the quantum duplex coding protocol is demonstrated using the H(V)-QZ$_N$ gate. As shown in Fig. 8, an electron as a quantum AO for duplexing coding takes the superposition of two paths $|\uparrow\rangle_e$ and $|\downarrow\rangle_e$ where the subscript e denotes the electron. In type I (Fig. 8(a)), the electron state $|\uparrow\,(\downarrow)\rangle_e$ or $|\downarrow\,(\uparrow)\rangle_e$ acts as the presence state $|1\rangle_{AO}$ or the absence state $|0\rangle_{AO}$ of the AO for the H(V)-QZ$_N$ gate. For counterfactuality, we setup the electron-photon interaction H(V)-MQZ$_N$ as shown in Fig. 9 where the quantum AO is in the superposition state

$$|\text{electron}\rangle_e = \alpha|\uparrow\rangle_e + \beta|\downarrow\rangle_e, \quad (20)$$

with $|\alpha|^2 + |\beta|^2 = 1$. The H(V)-MQZ$_N$ interaction collapses this quantum state by entangling and disentangling the electron-photon pair

$$|\phi_0\rangle_{ep} = |\text{electron}\rangle_e |H\,(V)\rangle_p \quad (21)$$

as follows:

$$|\phi_0\rangle_{ep} \to |\phi_1\rangle_{ep} = \alpha|\uparrow H\rangle_{ep} + \beta|\downarrow V\rangle_{ep} \quad (22)$$
$$\to |\phi_2\rangle_{ep} = |\uparrow\,(\downarrow)\rangle_e |H\,(V)\rangle_p, \quad (23)$$

unless the photon is absorbed by the electron with the probability

$$\left(1 - \Delta_0 \sin^2 \theta_N\right)^N \Delta_0 \quad (24)$$

where $\Delta_0 = |\alpha|^2 \left(|\beta|^2\right)$ is the probability that the electron is in the presence state for the H(V)-QZ$_N$ gate.

The second (first) term of $|\phi_1\rangle_{ep}$ is the outcome corresponding to the electron in the absence state for the H(V)-QZ$_N$ gate. Since this outcome is not counterfactual, it is discarded (absorbed) by the electron using the polarizing beam splitter PSB$^{H(V)}$ and the X operator. Hence, whenever the photon
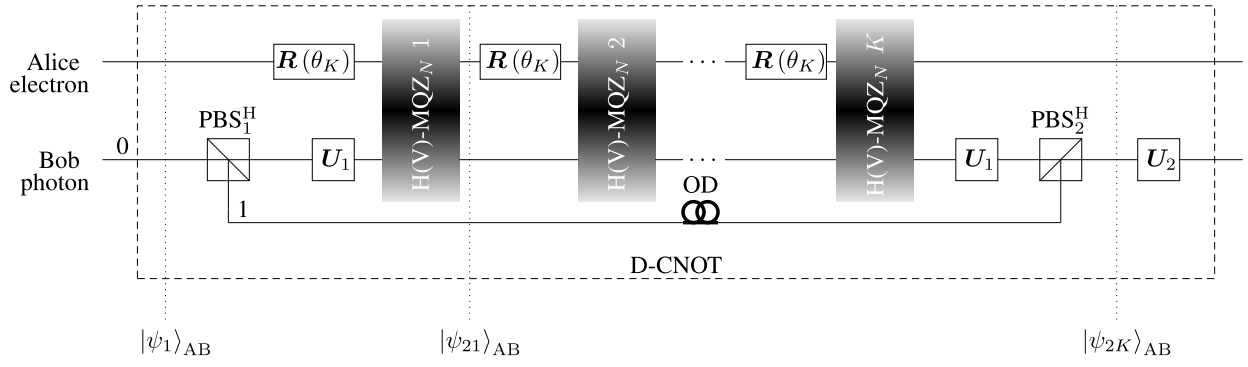
Fig. 10. A D-CNOT operation for Bell states when $b_2 = 0\,(1)$. Here, $\boldsymbol{R}\,(\theta_K)$ is a rotation operator of rotation angle θ_K where K is the number of H(V)-MQZ$_N$ gates. Initially, Alice and Bob have the maximally entangled state $|\psi_1\rangle_{AB}$, which is transformed by K sets of the θ_K rotation and MQZ gates successively to the separable state $|\psi_{2K}\rangle_{AB}$ in a controlled manner. Finally, the $\boldsymbol{U}_2$ operator is performed on the recombined photon to complete the D-CNOT operation.
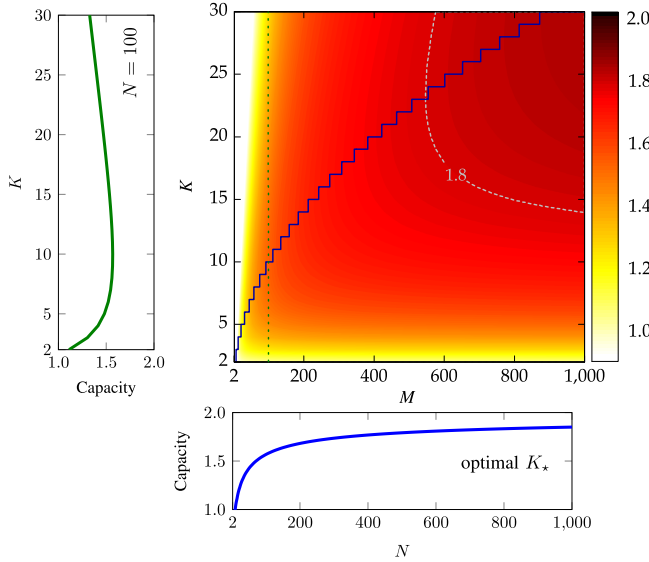

Fig. 11. Capacity C [bits/Bell-pair] of MQZ duplex coding as a function of N and K. Since the success probability ζ_c in (34) is concave in $K > 1$ for any positive integer N (see the left plot), there exists the optimal value (positive integer) of K that maximizes the capacity for a given N. The blue solid line is the trajectory of capacity as a function of N for the optimal values of K. The left plot depicts the capacity as a function of K when $N = 100$. We also plot the trajectory of (N, K) achieving the capacity of 1.8 bits/Bell-pair (white dashed line).

is found in the quantum channel, the electron absorbs it and becomes an erasure state, leading the MQZ gate to output no photon and electron (e.g., particles in the erasure state). To discard the factual (non-counterfactual) outcome $|V\,(H)\rangle_p$ of the H(V)-QZ$_N$ gate, we can simply use a photon detector after PBS$^{H(V)}$. Instead, we redirect this photon component to the quantum AO (followed by the σ_x operator) to be absorbed by the electron. This enables the protocol to abort nonlocally by discarding both the photon and the electron whenever its counterfactuality is broken.

To implement the D-CNOT operation for MQZ duplex coding, we cascade K H(V)-MQZ$_N$ gates, where Alice is equipped with the electron and Bob has the MQZ gates (see Fig. 10). Consider that

$$|0\rangle_A = |0\rangle_e, \tag{25}$$
$$|1\rangle_A = |1\rangle_e, \tag{26}$$

$$|0\rangle_B = |H\rangle_p, \tag{27}$$
$$|1\rangle_B = |V\rangle_p. \tag{28}$$

The MQZ duplex coding protocol takes the following steps to implement D-CNOT operation after encoding the classical information $b_1 b_2$.

1) Bob starts the protocol by separating the H and V components of the photon into two paths $|0\rangle_C$ and $|1\rangle_C$, respectively by using PBS^H. Bob locally applies the unitary operation $\boldsymbol{U}_1 = \boldsymbol{X}^{b_2}$ on the component of the photon in path state $|0\rangle_C$.

2) Alice applies the rotation operation $\boldsymbol{R}\,(\theta_K)$ on her qubit:

$$\boldsymbol{R}\,(\theta_K) = \begin{bmatrix} \cos\theta_K & -\sin\theta_K \\ \sin\theta_K & \cos\theta_K \end{bmatrix}. \tag{29}$$

The rotation gate $\boldsymbol{R}\,(\theta_K)$ transforms $|0\rangle_A$ and $|1\rangle_A$ as follows:

$$|0\rangle_A \rightarrow \cos\theta_K |0\rangle_A + \sin\theta_K |1\rangle_A \tag{30}$$
$$|1\rangle_A \rightarrow \cos\theta_K |1\rangle_A - \sin\theta_K |0\rangle_A. \tag{31}$$

3) Bob inputs the component of the photon in path $|0\rangle_C$ of the photon to H(V)-MQZ$_N$ gate for $b_2 = 0\,(1)$. Unless the photon is absorbed by the electron, it transforms the composite state of the Alice and Bob to $|\psi_{21}\rangle_{AB}$ in (32), as shown at the bottom of the next page, with the probability

$$\lambda_2 = \left(1 - \frac{1}{2}\cos^2\theta_K \sin^2\theta_N\right)^N \times \left(1 - \frac{1}{2}\sin^2\theta_K\right), \tag{33}$$

which tends to one as $N, K \rightarrow \infty$. Here $|0\rangle_C$ and $|1\rangle_C$ denote the optical path from PBS$_1^H$ to the H(V)-MQZ$_N$ gate and OD, respectively, and $|\Psi^\pm\rangle_{ABC} = |\Psi^\pm\rangle_{AB}|0\rangle_C$ and $|\Phi^\pm\rangle_{ABC} = |\Phi^\pm\rangle_{AB}|0\rangle_C$. Note that whenever the physical particle is travelled over the quantum channel between Alice and Bob, it is absorbed by the electron and the protocol declares an erasure.

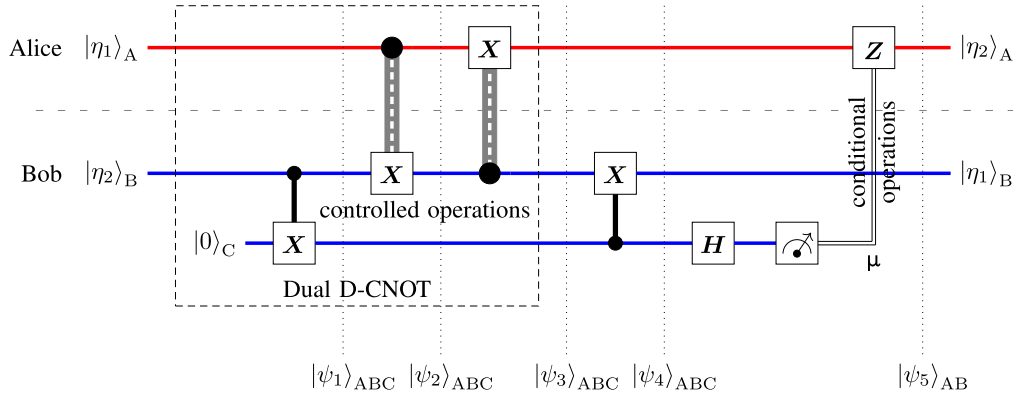4) Alice and Bob keep recurring the step 2) and step 3) for the remaining $(K - 1)$ H(V)-MQZ$_N$ gates unless the

Fig. 12. Quantum telexchanging for quantum information $|\eta_1\eta_2\rangle_{AB}$. Alice and Bob have an untangled pair of qubits $|\eta_1\rangle_A = \alpha|0\rangle_A + \beta|1\rangle_A$ and $|\eta_2\rangle_B = \gamma|0\rangle_B + \delta|1\rangle_B$ to communicate with each other. Bob starts the dual D-CNOT protocol by entangling his message $|\eta_2\rangle_B$ and ancilla $|0\rangle_C$ with the local CNOT operation. Alice and Bob perform the nonlocal operations on their composite state, which entangles and disentangles these remote parties successively to exchange their quantum information counterfactually. Then, Bob and Alice perform local operations to decode each quantum message. Specifically, Bob performs the CNOT operation followed by the Hadamard gate $\boldsymbol{H}$ to decode Alice's quantum message as $|\eta_1\rangle_B = \alpha|0\rangle_B + \beta|1\rangle_B$. Bob then announces his ancilla measurement $\mu \in \{0,1\}$ to Alice by classical communication. Using Bob's announcement, Alice finally performs the $\boldsymbol{Z}^\mu$ operator on her qubit to decode Bob's quantum message as $|\eta_2\rangle_A = \gamma|0\rangle_A + \delta|1\rangle_A$.

protocol declares the erasure with the probability $1 - \zeta_c$ where

$$\zeta_c = \lambda_2^K. \tag{34}$$

5) Bob applies $\boldsymbol{U}_1$ and recombines the H and V components of the photon. The encoded Bell pair $|\psi_1\rangle_{AB}$ is disentangled to $|\psi_{2K}\rangle_{ABC}$ as follows:

$$|\psi_{2K}\rangle_{ABC} : \begin{cases} |\Phi^\pm\rangle_{ABC} \rightarrow |0\rangle_A |\mp\rangle_B |0\rangle_C, \\ |\Psi^\pm\rangle_{ABC} \rightarrow |1\rangle_A |\pm\rangle_B |0\rangle_C. \end{cases} \tag{35}$$

6) Bob finally performs the $\boldsymbol{U}_2 = \boldsymbol{Z}^{1-b_2}$ operation on the component of the photon in path state $|0\rangle_C$ to complete the MQZ D-CNOT operation.

Alice measures the path of the electron to decode the classical information b_2. Bob first applies the Hadamard gate $\boldsymbol{H}$ to the photon, which transforms its polarization as

$$\boldsymbol{H}|+\rangle_B \rightarrow |H\rangle_p, \tag{36}$$
$$\boldsymbol{H}|-\rangle_B \rightarrow |V\rangle_p. \tag{37}$$

Bob measures the polarization of the existing photon to decode the classical information b_1. Table II shows the decoded messages corresponding to the measurement outcomes. The MQZ duplex coding creates a full-duplex form of the binary erasure channel with the erasure probability $1 - \zeta_c$. The bidirectional capacity C in bits/Bell-pair of the MQZ duplex coding is given by

$$C = 2\zeta_c \tag{38}$$

which tends to 2 bits/Bell-pair as $N, K \rightarrow \infty$ (see Fig. 11).[3]

---

[3]This protocol enables each party to achieve unidirectional capacity of ζ_c bits/Bell-pair in each direction simultaneously by using only one Bell-pair.

V. QUANTUM TELEXCHANGING

In this section, we develop a full-duplex quantum protocol to transfer quantum information in both directions simultaneously and counterfactually.

A. Protocol

Consider that Alice and Bob want to exchange their quantum states $|\eta_1\rangle_A$ and $|\eta_2\rangle_B$ simultaneously where

$$|\eta_1\rangle_A = \alpha|0\rangle_A + \beta|1\rangle_A, \tag{39}$$
$$|\eta_2\rangle_B = \gamma|0\rangle_B + \delta|1\rangle_B. \tag{40}$$

To transfer the quantum information in both directions at the same time, Alice and Bob perform the dual D-CNOT operation on their message qubits to entangle and disentangle them counterfactually. Bob starts the protocol by entangling his qubit $|\eta_2\rangle_B$ with his ancillary qubit $|0\rangle_C$ by performing the CNOT operation locally as shown in Fig. 12. Then, Alice and Bob have the separable composite state $|\psi_1\rangle_{ABC}$ as follows:

$$|\psi_1\rangle_{ABC} = |\eta_1\rangle_A (\gamma|00\rangle_{BC} + \delta|11\rangle_{BC}). \tag{41}$$

Alice and Bob perform the two nonlocal CNOT operations on their qubits. In the first CNOT operation, Alice's message qubit acts as a control qubit and Bob's message qubit acts as a target qubit. In the second CNOT operation, Alice's message qubit acts as a target qubit and Bob's message qubit acts as a control qubit. These nonlocal operations transform the composite state $|\psi_1\rangle_{ABC}$ as in (42)–(44), as shown at the bottom of the next page. Bob then applies the CNOT gate locally on his message and ancilla qubits to decode Alice's message state. It transforms $|\psi_3\rangle_{ABC}$ as follows:

$$|\psi_4\rangle_{ABC} = (\gamma|00\rangle_{AC} + \delta|11\rangle_{AC})$$
$$\times (\alpha|0\rangle_B + \beta|1\rangle_B). \tag{45}$$

$$|\psi_{21}\rangle_{AB} : \begin{cases} |\Phi^\pm\rangle_{ABC} \rightarrow \dfrac{1}{\sqrt{2}}\big(|000\rangle_{ABC} \pm \cos\theta_K |111\rangle_{ABC} \mp \sin\theta_K |011\rangle_{ABC}\big), \\ |\Psi^\pm\rangle_{ABC} \rightarrow \dfrac{1}{\sqrt{2}}\big(\pm|110\rangle_{ABC} + \cos\theta_K |011\rangle_{ABC} + \sin\theta_K |111\rangle_{ABC}\big). \end{cases} \tag{32}$$
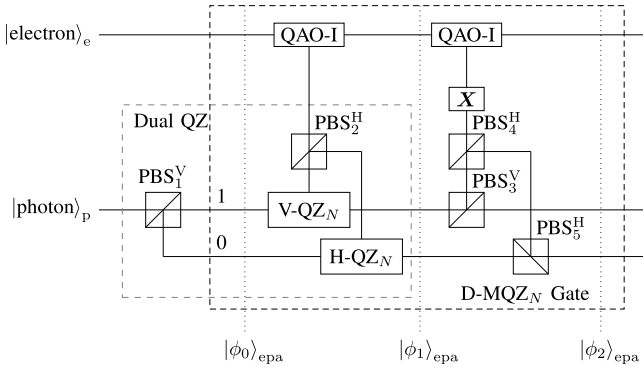
Fig. 13. A D-MQZ$_N$ interaction where the quantum AO (electron) gets entangled with the existing photon (unless absorbed by the electron) using the dual QZ gate. Initially, the photon is in the superposition state $|\text{photon}\rangle_p = \gamma |0\rangle_p + \delta |1\rangle_p$, which is entangled with the ancillary path state by PBS^H as $|\text{photon}\rangle_{pa} = \gamma |H0\rangle_{pa} + \delta |V1\rangle_{pa}$ to start the D-MQZ$_N$ interaction. Similar to the MQZ gate in Fig. 9, the D-MQZ$_N$ gate then transforms the electron-photon pair $|\phi_0\rangle_{epa}$ to $|\phi_2\rangle_{epa} = \gamma |\uparrow H0\rangle_{epa} + \delta |\downarrow V1\rangle_{epa}$ by using the blocking event only (unless the photon is absorbed by the electron).

To further disentangle Bob's ancilla and Alice's qubit, Bob applies the Hadamard gate $\boldsymbol{H}$ on his ancilla followed by measuring it in computational basis. Bob announces this measurement outcome $\mu \in \{0, 1\}$ to Alice by classical communication and Alice finally performs the $\boldsymbol{Z}^\mu$ operation on her qubit to decode Bob's message state as follows:

$$|\psi_5\rangle_{AB} = (\gamma |0\rangle_A + \delta |1\rangle_A)(\alpha |0\rangle_B + \beta |1\rangle_B)$$
$$= |\eta_2\rangle_A |\eta_1\rangle_B. \quad (46)$$

Whenever a physical particle is found in the quantum channel for the dual D-CNOT operation, the protocol discards it and declares an erasure of the quantum information $|\eta_1\eta_2\rangle_{AB}$.

B. MQZ-CQZ Telexchanging

In this section, the quantum telexchanging protocol is demonstrated using the H(V)-QZ$_N$ and H(V)-CQZ$_{M,N}$ gates. Fig. 13 shows the dual form of the MQZ gate in Fig. 9. For counterfacuality, this D-MQZ$_N$ gate works similarly to the H(V)-MQZ$_N$ gate. The only difference is that the superposition polarization state $|\text{photon}\rangle_p = \gamma |H\rangle_p + \delta |V\rangle_p$ of the input photon is entangled with the ancillary path state in the D-MQZ$_N$ gate as follows:

$$|\text{photon}\rangle_{pa} = \gamma |H0\rangle_{pa} + \delta |V1\rangle_{pa} \quad (47)$$

where the ancilla states $|0\rangle_a$ and $|1\rangle_a$ show the paths for the H- and V-QZ gates, respectively. The D-MQZ$_N$ gate transforms the electron-photon pair

$$|\phi_0\rangle_{epa} = |\text{electron}\rangle_e |\text{photon}\rangle_{pa} \quad (48)$$

as follows:

$$|\phi_0\rangle_{epa} \rightarrow |\phi_1\rangle_{epa} = \alpha\gamma |\uparrow H0\rangle_{epa} + \beta\gamma |\downarrow V0\rangle_{epa}$$

$$+ \alpha\delta |\uparrow H1\rangle_{epa} + \beta\delta |\downarrow V1\rangle_{epa}$$
$$\rightarrow |\phi_2\rangle_{epa} = \gamma |\uparrow H0\rangle_{epa} + \delta |\downarrow V1\rangle_{epa} \quad (49)$$

unless the photon is absorbed by the electron with the probability

$$\left(1 - \Delta_1 \sin^2 \theta_N\right)^N \Delta_1, \quad (50)$$

where $\Delta_1 = |\alpha\gamma|^2 + |\beta\delta|^2$ is the probability that the electron is in the presence state for the QZ gates in both paths.

For MQZ-CQZ quantum telexchanging, Alice and Bob initially have an untangled pair of quantum information $|\eta_1\rangle_A$ and $|\eta_2\rangle_B$ prepared in the electron and photon, respectively, where we consider (25)–(28) again. Bob starts the protocol by throwing his photon towards PBS^H to entangle the polarization state $|\text{photon}\rangle_B$ with the ancillary path state $|0\rangle_C$ as shown in Fig. 14. Then, Alice and Bob have the composite state $|\psi_1\rangle_{ABC}$ in (41). To implement the dual D-CNOT operation in Fig. 12, Alice and Bob first entangle their qubits counterfactually by using the dual CQZ gate and then perform K D-MQZ$_N$ gates for controlled disentanglement (see Fig. 14). The MQZ-CQZ telexchanging takes the following steps to device the dual D-CNOT operation after preparing the message states.

1) Alice and Bob start the dual D-CNOT protocol by entangling their message states $|\text{electron}\rangle_A$ and $|\text{photon}\rangle_B$ counterfactually where Alice's message state $|\text{electron}\rangle_A$ acts as a quantum AO and Bob is equipped with the dual CQZ gate. Unless the photon is absorbed by the electron or discarded at the detector in the dual CQZ gate, this counterfactual entanglement transforms the encoded state $|\psi_1\rangle_{ABC}$ to $|\psi_2\rangle_{ABC}$ in (44) with the probability

$$\lambda_3 = \left(1 - |\alpha|^2 \sin^2 \theta_M\right)^M$$
$$\prod_{m=1}^{M} \left[1 - |\beta|^2 \sin^2 (m\theta_M) \sin^2 \theta_N\right]^N, \quad (51)$$

which tends to one as $M, N \rightarrow \infty$ [64].

2) Bob applies PBS^H in each path of the photon to separate the H and V components of the photon and performs the $\boldsymbol{U}_3$ operation locally where

$$\boldsymbol{U}_3 = \boldsymbol{I} \otimes \left(|0\rangle_C\langle 0| + |3\rangle_C\langle 3|\right) + \boldsymbol{X} \otimes |1\rangle_C\langle 1|$$
$$+ \boldsymbol{Z} \otimes |2\rangle_C\langle 2|. \quad (52)$$

3) Alice applies the rotation operation $\boldsymbol{R}(\theta_K)$ on her qubit and Bob applies the D-MQZ gate on the components of the photon in path states $|0\rangle_C$ and $|1\rangle_C$. Unless the photon is discarded in the D-MQZ gate, the D-MQZ gate transforms $|\psi_2\rangle_{ABC}$ as follows

$$|\psi_{21}\rangle_{ABC} = \alpha\gamma |000\rangle_{ABC} + \beta\delta |111\rangle_{ABC}$$
$$+ \beta\gamma \sin \theta_K |012\rangle_{ABC}$$

$$|\psi_1\rangle_{ABC} \rightarrow |\psi_2\rangle_{ABC} = \alpha\gamma |000\rangle_{ABC} + \alpha\delta |011\rangle_{ABC} + \beta\gamma |110\rangle_{ABC} + \beta\delta |101\rangle_{ABC}, \quad (42)$$

$$\rightarrow |\psi_3\rangle_{ABC} = \alpha\gamma |000\rangle_{ABC} + \alpha\delta |111\rangle_{ABC} + \beta\gamma |010\rangle_{ABC} + \beta\delta |101\rangle_{ABC} \quad (43)$$

$$= \gamma |00\rangle_{AC} (\alpha |0\rangle_B + \beta |1\rangle_B) + \delta |11\rangle_{AC} (\alpha |1\rangle_B + \beta |0\rangle_B). \quad (44)$$
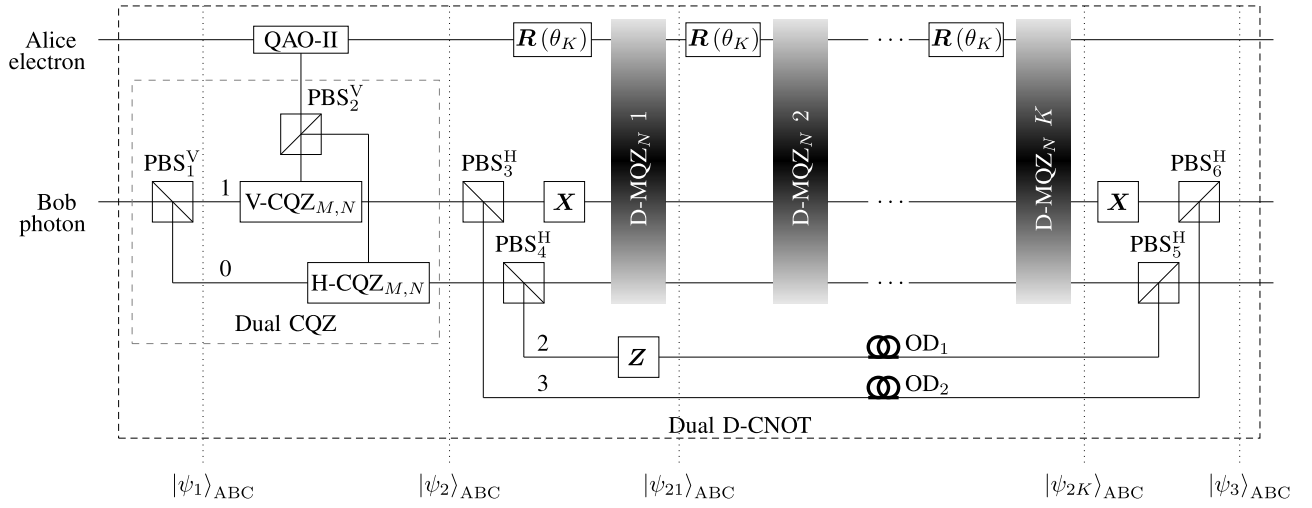
Fig. 14. A dual D-CNOT operation for an unknown pair of quantum states. Initially, Alice and Bob have an untangled pair $|\eta_1\eta_2\rangle_{\mathrm{AB}}$ of the electron and photon. This message pair is entangled by the dual CQZ gate and disentangled by K rounds of the θ_K rotation and D-MQZ$_N$ gates counterfactually in a controlled manner. Finally, Bob applies the X gate on the photon component in path $|1\rangle_C$ and recombines the respective components of the photon to complete the dual D-CNOT operation.
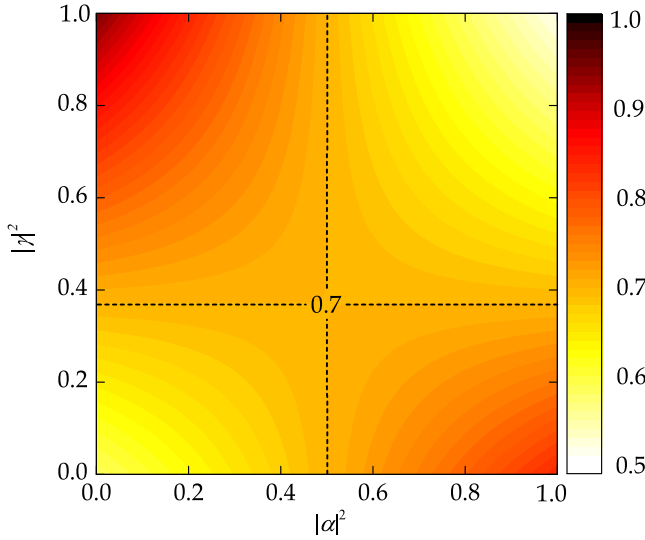

Fig. 15. Transfer efficiency (fidelity) ζ_q for the MQZ-CQZ telexchanging as a function of $|\alpha|^2$ and $|\gamma|^2$ when $N = 100$ and $M_\star = K_\star = 10$ where $M_\star$ and $K_\star$ are the optimal values that maximize ζ_q for given N such that $M_\star = \arg\max_M \zeta_3$ and $K_\star = \arg\max_K \zeta_4^K$. When $|\alpha|^2 = 1/2$, the transfer efficiency is equal to $\zeta_q = 0.659$ independent of the message states (black dashed line). We can see that ζ_q increases as $\Delta_1 \to 0$ (the message states are collapsing to the classical information). When $N = 100$, the maximum efficiency is equal to $\zeta_q = 0.903$ for $|\alpha|^2 = 0$ and $|\gamma|^2 = 1$.

$$- \beta\gamma\cos\theta_K |112\rangle_{\mathrm{ABC}}$$
$$+ \alpha\delta\cos\theta_K |013\rangle_{\mathrm{ABC}}$$
$$+ \alpha\delta\sin\theta_K |113\rangle_{\mathrm{ABC}} \quad (53)$$

with the probability

$$\lambda_4 = \left(1 - \Delta_1 \cos^2\theta_K \sin^2\theta_N\right)^N$$
$$\left(1 - \Delta_1 \sin^2\theta_K\right), \quad (54)$$

which tends to one as $N, K \to \infty$.

4) Alice and Bob keep repeating step 3) for the remaining $K - 1$ D-MQZ gates. The remaining $K - 1$ D-MQZ gates transform the composite state $|\psi_{21}\rangle$ to $|\psi_{2K}\rangle$ as

follows:

$$|\psi_{2K}\rangle_{\mathrm{ABC}} = \alpha\gamma |000\rangle_{\mathrm{ABC}} + \beta\delta |111\rangle_{\mathrm{ABC}}$$
$$+ \beta\gamma |012\rangle_{\mathrm{ABC}} + \alpha\delta |113\rangle_{\mathrm{ABC}}, \quad (55)$$

unless the photon is discarded in the dual D-CNOT operation with the probability $1 - \zeta_q$ where

$$\zeta_q = \lambda_3 \lambda_4^K. \quad (56)$$

Whenever the physical particle is transmitted over the quantum channel between Alice and Bob, the protocol declares an erasure of the quantum message $|\eta_1\eta_2\rangle_{\mathrm{AB}}$.

5) Bob applies U_4 on his photon and recombines the respective components of the photon to complete the dual D-CNOT operation ($|\psi_3\rangle_{\mathrm{ABC}}$) where

$$U_4 = I \otimes \left(|0\rangle_C\langle 0| + |2\rangle_C\langle 2| + |3\rangle_C\langle 3|\right)$$
$$+ X \otimes |1\rangle_C\langle 1|. \quad (57)$$

This MQZ-CQZ telexchanging for quantum information creates a full-duplex form of the quantum erasure channel [70] with the erasure probability $1 - \zeta_q$ as follows:

$$|\eta_1\eta_2\rangle_{\mathrm{AB}} \to \mathcal{N}\left(|\eta_1\eta_2\rangle_{\mathrm{AB}}\right)$$
$$= \zeta_q |\eta_1\eta_2\rangle_{\mathrm{BA}}\langle\eta_1\eta_2| + (1 - \zeta_q)|\varepsilon\rangle_{\mathrm{BA}}\langle\varepsilon| \quad (58)$$

where $\mathcal{N}$ denotes the full-duplex quantum erasure channel formed by the protocol and $|\varepsilon\rangle_{\mathrm{BA}}$ is the erasure state orthogonal and independent to the message state $|\eta_1\eta_2\rangle_{\mathrm{AB}}$. The transfer efficiency ζ_q can be also viewed as the fidelity

$$F = \langle\eta_1\eta_2|\mathcal{N}|\eta_1\eta_2\rangle_{\mathrm{AB}}, \quad (59)$$

which depends on the message state $|\eta_1\eta_2\rangle_{\mathrm{AB}}$ in general. Since $\Delta_1 = 1/2$ if $|\alpha|^2 = |\beta|^2 = 1/2$, this dependence vanishes when Alice's message $|\eta_1\rangle_{\mathrm{A}}$ is in the superposition state of equiprobable $|0\rangle_{\mathrm{A}}$ and $|1\rangle_{\mathrm{A}}$ (see Fig. 15). The quantum capacity Q in qubits/electron-photon for the MQZ-CQZ telexchanging is given by

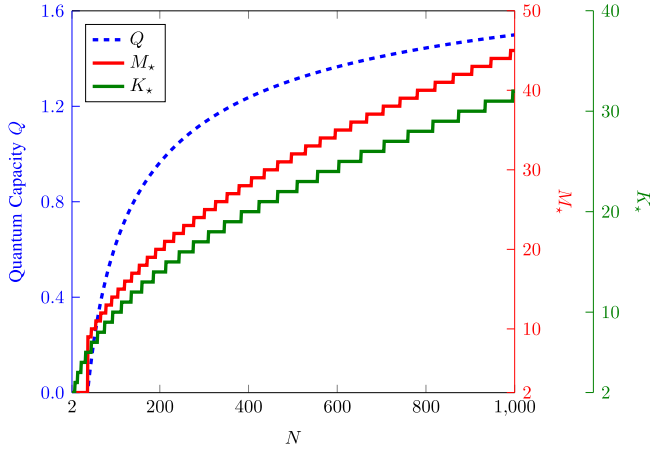$$Q = 2\max\{0, 2\zeta_q - 1\} \quad (60)$$

Fig. 16. Quantum capacity Q [qubits/electron-photon], $M_\star$, and $K_\star$ for the MQZ-CQZ telexchanging as a function of N when $|\alpha|^2 = |\beta|^2 = 1/2$ where $M_\star$ and $K_\star$ are the optimal values of M and K that maximize the quantum capacity Q or equivalently the transfer efficiency ζ_q for given N as in Fig. 15. The 50% efficiency ($Q = 1$ qubit/electron-photon) is attained when $N = 218$ with $M_\star = 21$ and $K_\star = 15$.
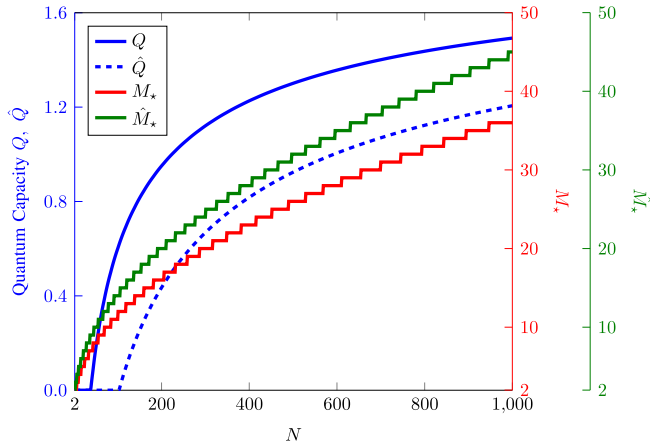

Fig. 17. Quantum capacity and the optimal value of M for the quantum telexchanging and the counterfactual state exchange protocol presented in [17] where K is simply set to $M_\star$ for the MQZ-CQZ telexchanging protocol. Here $\hat{Q}$ and $\hat{M}_\star$ denote the quantum capacity and the optimal value of M for the protocol presented in [17].

tending to 2 qubits/electron-photon as $K, M, N \to \infty$ (see Fig. 16).

Recently, the counterfactual quantum state exchange has been demonstrated by using the CQZ gates along with time-bin device [17]. Fig. 17 shows the comparison between quantum telexchanging (our scheme) and the protocol proposed in [17] in terms of quantum capacity and the optimal value of M as a function of N when $|\alpha|^2 = |\gamma|^2 = 1/2$. Here Q is the quantum capacity achieved by MQZ-CQZ telexchanging with $M = K = M_\star$ and $\hat{Q}$ is the quantum capacity achieved by the protocol in [17] with $M = \hat{M}_\star$. It can be seen that $Q > \hat{Q}$ whereas $M_\star < \hat{M}_\star$ for all values of N, which shows that our protocol gives better performance while using fewer resources (number of outer cycles).

VI. Discussion

A. Nonlocality in Counterfactual Communication

Counterfactual quantum communication allows communicating parties, Alice and Bob, to transfer information without

transmitting any physical particle over the quantum channel. However, it may be unclear what is nonlocal in counterfactual communication [47], [71]. Recently, it has been shown that the counterfactual quantum communication is the application of the quantum Cheshire Cat effect [25], which states that properties such as the spin of an electron can be disembodied from the physical particles [72], [73]. Due to the quantum Cheshire Cat effect, properties of the physical particle can be affected by external actions even if the physical particle is not present there.

To transmit classical information in a counterfactual manner, Alice controls the presence or absence of an AO in a classical manner. For $\mathsf{b} = 1$, the presence of an AO is similar to measuring the photon. In case the photon is found in the transmission channel, it will be absorbed by the AO. Here it can be seen that in each outer cycle, the measurement frequency $f_1 = N$ for $\mathsf{b} = 1$. For $\mathsf{b} = 0$, the absence of an AO is similar to not performing any measurement on the photon. However, the photon component in the inner cycles ends up at detector D in Fig. 2, which shows that in each outer cycle, the measurement frequency $f_1 = 1$ for $\mathsf{b} = 0$. Since quantum measurements collapse the state of the system, it can be seen that the quantum Cheshire Cat effect [25] and measurement frequency f_1 carry information in counterfactual quantum communication where f_1 after M outer cycles is given as [47]

$$f_1 = \begin{cases} M, & \text{for } \mathsf{b} = 0, \\ MN, & \text{for } \mathsf{b} = 1. \end{cases} \quad (61)$$

Similarly, in D-CNOT and dual D-CNOT gates, the measurement frequency f_2 is given as

$$f_2 = \begin{cases} K, & \text{for non-blocking events,} \\ KN, & \text{for blocking events.} \end{cases} \quad (62)$$

In D-CNOT gates, Bob starts the protocol by separating the H and V photon components in path states $|0\rangle_C$ and $|1\rangle_C$, respectively, whereas Alice performs the $\boldsymbol{R}(\theta_K)$ rotation operator on her qubit. Note that the MQZ gates output the photon corresponding to the blocking events only. Unless the electron absorbs the photon, the MQZ gates restrict the rotation of the electron corresponding to the photon component in path state $|0\rangle_C$. However, the V photon component in path state $|1\rangle_C$ does not interact with the electron; each $\boldsymbol{R}(\theta_K)$ operator rotates the electron state by an angle θ_K (see (32)). Following a similar procedure for the dual D-CNOT gate, it can be seen that the measurement frequency f_2 and the controlled rotation carry the information in D-CNOT and dual D-CNOT gates.

B. Comparison

The quantum duplex coding and telexchanging are full-duplex counterparts to the quantum superdense coding and teleportation, respectively. The quantum superdense coding utilizes a striking nonclassical property of Bell states, which sends two bits of classical information in one qubit, whereas quantum teleportation enables remote parties to transfer quantum information with two-bit classical information by using the preshared quantum entanglement. The quantum duplex

coding and telexchanging have the following advantages over these quantum communication protocols.

- Quantum superdense coding is a simplex protocol to allow the communication of a two-bit classical message in one direction only. In contrast, quantum duplex coding allows the full-duplex communication by means of the nonlocal D-CNOT operation. Although both the protocols transmit 2 bits/Bell-pair, the main advantage of the quantum duplex coding is to transfer classical information in both directions simultaneously.
- Quantum teleportation utilizes a prior entanglement to send one qubit of a quantum message. In contrast, quantum telexchanging enables communicating parties to transmit quantum information without preshared entanglement. To exchange a qubit of quantum information by using quantum teleportation, remote parties need two Bell pairs at the cost of four qubits and four bits of classical information. In contrast, the quantum telexchanging enables remote parties to exchange one qubit quantum information at the cost of one ancilla qubit and one bit of classical information. To ensure the conterfactuality of the protocol, the quantum capacity of quantum telexchanging is limited to Q in (60) due to the erasure probability $1 - \zeta_q$.

VII. CONCLUSION

We have put forth the new quantum communication protocols that achieve both full duplexity and counterfactuality for the classical as well as quantum information. Using the preshared entanglement and the nonlocal D-CNOT operation (counterfactual disentanglement), this unique quantum protocol allows remote parties to swap a one-bit of classical information simultaneously without transmitting any physical particle over the channel. We have generalized this counterfactual duplex communication framework for the quantum information by devising the dual D-CNOT operation (counterfactual entanglement followed by disentanglement in a distributed way) along with local operations and one-bit announcement of classical information. The communication without transmitting any physical particle over the channel can further provide inherent security advantages over the most of eavesdropping attacks such as the photon-number splitting attack and the intercept-and-resend attack. The future work can be done to extend the quantum communication protocols to transfer the information in both directions simultaneously, counterfactually—and *securely*.

REFERENCES

[1] M. Giordani, M. Polese, M. Mezzavilla, S. Rangan, and M. Zorzi, "Toward 6G networks: Use cases and technologies," *IEEE Commun. Mag.*, vol. 58, no. 3, pp. 55–61, Mar. 2020.

[2] C. Wang and A. Rahman, "Quantum-enabled 6G wireless networks: Opportunities and challenges," *IEEE Wireless Commun.*, vol. 29, no. 1, pp. 58–69, Feb. 2022.

[3] F. Zaman, A. Farooq, M. A. Ullah, H. Jung, H. Shin, and M. Z. Win, "Quantum machine intelligence for 6G URLLC," *IEEE Wireless Commun.*, vol. 30, no. 2, pp. 22–30, Apr. 2023.

[4] S. K. Sharma, T. E. Bogale, L. B. Le, S. Chatzinotas, X. Wang, and B. Ottersten, "Dynamic spectrum sharing in 5G wireless networks with full-duplex technology: Recent advances and research challenges," *IEEE Commun. Surveys Tuts.*, vol. 20, no. 1, pp. 674–707, 1st Quart., 2018.

[5] I. P. Roberts, J. G. Andrews, H. B. Jain, and S. Vishwanath, "Millimeter-wave full duplex radios: New challenges and techniques," *IEEE Wireless Commun.*, vol. 28, no. 1, pp. 36–43, Feb. 2021.

[6] N. Nomikos, T. Charalambous, D. Vouyioukas, and G. K. Karagiannidis, "When buffer-aided relaying meets full duplex and NOMA," *IEEE Wireless Commun.*, vol. 28, no. 1, pp. 68–73, Feb. 2021.

[7] Z. Xiao and Y. Zeng, "Waveform design and performance analysis for full-duplex integrated sensing and communication," *IEEE J. Sel. Areas Commun.*, vol. 40, no. 6, pp. 1823–1837, Jun. 2022.

[8] G. C. Alexandropoulos, M. A. Islam, and B. Smida, "Full duplex massive MIMO architectures: Recent advances, applications, and future directions," 2022, *arXiv:2205.08393*.

[9] Z. Zhang, K. Long, A. V. Vasilakos, and L. Hanzo, "Full-duplex wireless communications: Challenges, solutions, and future research directions," *Proc. IEEE*, vol. 104, no. 7, pp. 1369–1409, Jul. 2016.

[10] H. Wang, Y. Q. Zhang, X. F. Liu, and Y. P. Hu, "Efficient quantum dialogue using entangled states and entanglement swapping without information leakage," *Quantum Inf. Process.*, vol. 15, no. 6, pp. 2593–2603, Mar. 2016.

[11] A. Maitra, "Measurement device-independent quantum dialogue," *Quantum Inf. Process.*, vol. 16, no. 12, pp. 1–15, Nov. 2017.

[12] L. Zhou, Y.-B. Sheng, and G.-L. Long, "Device-independent quantum secure direct communication against collective attacks," *Sci. Bull.*, vol. 65, no. 1, pp. 12–20, Jan. 2020.

[13] W. Zhang, D.-S. Ding, Y.-B. Sheng, L. Zhou, B.-S. Shi, and G.-C. Guo, "Quantum secure direct communication with quantum memory," *Phys. Rev. Lett.*, vol. 118, no. 22, May 2017, Art. no. 220501.

[14] Y. Lee, R. Takagi, H. Yamasaki, G. Adesso, and S. Lee, "State exchange with quantum side information," *Phys. Rev. Lett.*, vol. 122, no. 1, Jan. 2019, Art. no. 010502.

[15] Y. Lee, H. Yamasaki, G. Adesso, and S. Lee, "One-shot quantum state exchange," *Phys. Rev. A, Gen. Phys.*, vol. 100, no. 4, Oct. 2019, Art. no. 042306.

[16] J. Oppenheim and A. Winter, "Uncommon information (the cost of exchanging a quantum state)," 2005, *arXiv:quant-ph/0511082*.

[17] Z.-H. Li, M. Al-Amri, X.-H. Yang, and M. S. Zubairy, "Counterfactual exchange of unknown quantum states," *Phys. Rev. A, Gen. Phys.*, vol. 100, no. 2, Aug. 2019, Art. no. 022110.

[18] A. Farooq, J. U. Rehman, Y. Jeong, J. S. Kim, and H. Shin, "Tightening monogamy and polygamy inequalities of multiqubit entanglement," *Sci. Rep.*, vol. 9, no. 1, p. 3314, Mar. 2019.

[19] R. Horodecki, P. Horodecki, M. Horodecki, and K. Horodecki, "Quantum entanglement," *Rev. Mod. Phys.*, vol. 81, no. 2, pp. 865–942, Jun. 2009.

[20] J. T. Barreiro, N. K. Langford, N. A. Peters, and P. G. Kwiat, "Generation of hyperentangled photon pairs," *Phys. Rev. Lett.*, vol. 95, no. 26, Dec. 2005, Art. no. 260501.

[21] H. Salih, Z.-H. Li, M. Al-Amri, and M. S. Zubairy, "Protocol for direct counterfactual quantum communication," *Phys. Rev. Lett.*, vol. 110, no. 17, Apr. 2013, Art. no. 170502.

[22] Y. Aharonov and L. Vaidman, "Modification of counterfactual communication protocols that eliminates weak particle traces," *Phys. Rev. A, Gen. Phys.*, vol. 99, no. 1, Jan. 2019, Art. no. 010103.

[23] Z.-H. Li, M. Al-Amri, and M. S. Zubairy, "Direct quantum communication with almost invisible photons," *Phys. Rev. A, Gen. Phys.*, vol. 89, no. 5, May 2014, Art. no. 052334.

[24] Y. Cao et al., "Direct counterfactual communication via quantum Zeno effect," *Proc. Nat. Acad. Sci. USA*, vol. 114, no. 19, pp. 4920–4924, May 2017.

[25] Y. Aharonov, E. Cohen, and S. Popescu, "A dynamical quantum Cheshire Cat effect and implications for counterfactual communication," *Nature Commun.*, vol. 12, no. 1, pp. 1–8, Aug. 2021.

[26] Z.-H. Li, S.-Y. Feng, M. Al-Amri, and M. S. Zubairy, "Direct counterfactual quantum communication protocol beyond single photon source," 2022, *arXiv:2202.03935*.

[27] O. Hosten, M. T. Rakher, J. T. Barreiro, N. A. Peters, and P. G. Kwiat, "Counterfactual quantum computation through quantum interrogation," *Nature*, vol. 439, no. 7079, pp. 949–952, Feb. 2006.

[28] F. Kong et al., "Experimental realization of high-efficiency counterfactual computation," *Phys. Rev. Lett.*, vol. 115, no. 8, Aug. 2015, Art. no. 080501.

[29] G. Mitchison, R. Jozsa, and S. Popescu, "Sequential weak measurement," *Phys. Rev. A, Gen. Phys.*, vol. 76, no. 6, Dec. 2007, Art. no. 062105.

[30] F. Zaman, H. Shin, and M. Z. Win, "Counterfactual concealed telecomputation," 2020, *arXiv:2012.04948*.

[31] T.-G. Noh, "Counterfactual quantum cryptography," *Phys. Rev. Lett.*, vol. 103, no. 23, Dec. 2009, Art. no. 230501.

[32] Z.-Q. Yin et al., "Counterfactual quantum cryptography based on weak coherent states," *Phys. Rev. A, Gen. Phys.*, vol. 86, no. 2, Aug. 2012, Art. no. 022313.

[33] H. Salih, "Tripartite counterfactual quantum cryptography," *Phys. Rev. A, Gen. Phys.*, vol. 90, no. 1, Jul. 2014, Art. no. 012333.

[34] Y. Sun and Q.-Y. Wen, "Counterfactual quantum key distribution with high efficiency," *Phys. Rev. A, Gen. Phys.*, vol. 82, no. 5, Nov. 2010, Art. no. 052318.

[35] Y. Liu et al., "Experimental demonstration of counterfactual quantum communication," *Phys. Rev. Lett.*, vol. 109, no. 3, Jul. 2012, Art. no. 030501.

[36] F. Zaman, Y. Jeong, and H. Shin, "Man in the middle attack in counterfactual quantum key distribution," in *Proc. Korean Inst. Commun. Inf. Sci. (KICS) Autumn Conf.*, Nov. 2018, pp. 105–106.

[37] S. N. Paing, F. Zaman, and H. Shin, "Counterfactual quantum private comparison," in *Proc. Korean Inst. Commun. Inf. Sci. (KICS) Winter Conf.*, Feb. 2022, pp. 651–653.

[38] A. Elitzur and L. Vaidman, "Quantum mechanical interaction-free measurement," *Found. Phys.*, vol. 23, no. 76, pp. 987–997, Jul. 1993.

[39] P. Kwiat, H. Weinfurter, T. Herzog, A. Zeilinger, and M. A. Kasevich, "Interaction-free measurement," *Phys. Rev. Lett.*, vol. 74, no. 24, p. 4763, Nov. 1995.

[40] I. A. Calafell et al., "Trace-free counterfactual communication with a nanophotonic processor," *NPJ Quantum Inf.*, vol. 5, no. 1, pp. 1–5, Jul. 2019.

[41] Q. Guo, L.-Y. Cheng, L. Chen, H.-F. Wang, and S. Zhang, "Counterfactual quantum-information transfer without transmitting any physical particles," *Sci. Rep.*, vol. 5, no. 1, p. 8416, Feb. 2015.

[42] Z.-H. Li, M. Al-Amri, and M. S. Zubairy, "Direct counterfactual transmission of a quantum state," *Phys. Rev. A, Gen. Phys.*, vol. 92, no. 5, Nov. 2015, Art. no. 052315.

[43] H. Salih, "Protocol for counterfactually transporting an unknown qubit," *Frontiers Phys.*, vol. 3, p. 94, Jan. 2016.

[44] S. N. Paing, F. Zaman, and H. Shin, "Counterfactual controlled quantum teleportaion," in *Proc. Korean Inst. Commun. Inf. Sci. (KICS) Winter Conf.*, Feb. 2021, pp. 542–543.

[45] H. Salih, J. R. Hance, W. McCutcheon, T. Rudolph, and J. Rarity, "Deterministic teleportation and universal computation without particle exchange," 2020, *arXiv:2009.05564*.

[46] F. Zaman and H. Shin, "Counterfactual swap gates," in *Proc. Korean Inst. Commun. Inf. Sci. (KICS) Winter Conf.*, Feb. 2021, pp. 389–390.

[47] F. Zaman, K. Lee, and H. Shin, "Information carrier and resource optimization of counterfactual quantum communication," *Quantum Inf. Process.*, vol. 20, no. 5, pp. 1–10, May 2021.

[48] S. D. Bartlett, T. Rudolph, and R. W. Spekkens, "Reference frames, superselection rules, and quantum information," *Rev. Mod. Phys.*, vol. 79, no. 2, pp. 555–609, Apr. 2007.

[49] E. O. Ilo-Okeke, L. Tessler, J. P. Dowling, and T. Byrnes, "Remote quantum clock synchronization without synchronized clocks," *NPJ Quantum Inf.*, vol. 4, no. 1, pp. 1–5, Aug. 2018.

[50] A. S. Fletcher, P. W. Shor, and M. Z. Win, "Optimum quantum error recovery using semidefinite programming," *Phys. Rev. A, Gen. Phys.*, vol. 75, no. 1, Jan. 2007, Art. no. 012338.

[51] A. S. Fletcher, P. W. Shor, and M. Z. Win, "Structured near-optimal channel-adapted quantum error correction," *Phys. Rev. A, Gen. Phys.*, vol. 77, no. 1, Jan. 2008, Art. no. 012320.

[52] A. S. Fletcher, P. W. Shor, and M. Z. Win, "Channel-adapted quantum error correction for the amplitude damping channel," *IEEE Trans. Inf. Theory*, vol. 54, no. 12, pp. 5705–5718, Dec. 2008.

[53] K. Boström and T. Felbinger, "Deterministic secure direct communication using entanglement," *Phys. Rev. Lett.*, vol. 89, no. 18, Oct. 2002, Art. no. 187902.

[54] J.-Y. Hu et al., "Experimental quantum secure direct communication with single photons," *Light, Sci. Appl.*, vol. 5, no. 9, Apr. 2016, Art. no. e16144.

[55] S. Qaisar, J. U. Rehman, Y. Jeong, and H. Shin, "Practical deterministic secure quantum communication in a lossy channel," *Prog. Theor. Exp. Phys.*, vol. 2017, no. 4, Apr. 2017, Art. no. 041A01.

[56] L. Ruan, W. Dai, and M. Z. Win, "Adaptive recurrence quantum entanglement distillation for two-Kraus-operator channels," *Phys. Rev. A, Gen. Phys.*, vol. 97, no. 5, May 2018, Art. no. 052332.

[57] A. Khan, A. Farooq, Y. Jeong, and H. Shin, "Distribution of entanglement in multipartite systems," *Quantum Inf. Process.*, vol. 18, no. 2, p. 60, Jan. 2019.

[58] W. K. Wootters and W. H. Zurek, "A single quantum cannot be cloned," *Nature*, vol. 299, no. 5886, pp. 802–803, Oct. 1982.

[59] Z.-H. Li, L. Wang, J. Xu, Y. Yang, M. Al-Amri, and M. S. Zubairy, "Counterfactual trojan horse attack," *Phys. Rev. A, Gen. Phys.*, vol. 101, no. 2, Feb. 2020, Art. no. 022336.

[60] M. A. Ullah, S. N. Paing, and H. Shin, "Noise-robust quantum teleportation with counterfactual communication," *IEEE Access*, vol. 10, pp. 61484–61493, 2022.

[61] Q. Guo, L.-Y. Cheng, L. Chen, H.-F. Wang, and S. Zhang, "Counterfactual entanglement distribution without transmitting any particles," *Opt. Exp.*, vol. 22, no. 8, pp. 8970–8984, Apr. 2014.

[62] Y. Chen, X. Gu, D. Jiang, L. Xie, and L. Chen, "Tripartite counterfactual entanglement distribution," *Opt. Exp.*, vol. 23, no. 16, pp. 21193–21203, Aug. 2015.

[63] Y. Chen, D. Jian, X. Gu, L. Xie, and L. Chen, "Counterfactual entanglement distribution using quantum dot spins," *J. Opt. Soc. Amer. B, Opt. Phys.*, vol. 33, no. 4, pp. 663–669, Jan. 2016.

[64] F. Zaman, Y. Jeong, and H. Shin, "Counterfactual bell-state analysis," *Sci. Rep.*, vol. 8, no. 1, p. 14641, Oct. 2018.

[65] F. Zaman, E.-K. Hong, and H. Shin, "Local distinguishability of bell-type states," *Quantum Inf. Process.*, vol. 20, no. 5, pp. 1–12, May 2021.

[66] Q. Guo, S. Zhai, L.-Y. Cheng, H.-F. Wang, and S. Zhang, "Counterfactual quantum cloning without transmitting any physical particles," *Phys. Rev. A, Gen. Phys.*, vol. 96, no. 5, Nov. 2017, Art. no. 052335.

[67] W. M. Itano, D. J. Heinzen, J. J. Bollinger, and D. Wineland, "Quantum Zeno effect," *Phys. Rev. A, Gen. Phys.*, vol. 41, no. 5, p. 2295, Mar. 1990.

[68] F. Zaman, Y. Jeong, and H. Shin, "Dual quantum Zeno superdense coding," *Sci. Rep.*, vol. 9, no. 1, p. 11193, Aug. 2019.

[69] T. M. Cover and J. A. Thomas, *Elements of Information Theory*. New York, NY, USA: Wiley, 2012.

[70] C. H. Bennett, D. P. DiVincenzo, and J. A. Smolin, "Capacities of quantum erasure channels," *Phys. Rev. Lett.*, vol. 78, no. 16, pp. 3217–3220, Apr. 1997.

[71] Y. Aharonov and D. Rohrlich, "What is nonlocal in counterfactual quantum communication?" *Phys. Rev. Lett.*, vol. 125, no. 26, Dec. 2020, Art. no. 260401.

[72] Y. Aharonov, S. Popescu, D. Rohrlich, and P. Skrzypczyk, "Quantum Cheshire Cats," *New J. Phys.*, vol. 15, no. 11, Nov. 2013, Art. no. 113015.

[73] T. Denkmayr et al., "Observation of a quantum Cheshire Cat in a matter-wave interferometer experiment," *Nature Commun.*, vol. 5, no. 1, pp. 1–7, Jul. 2014.

Fakhar Zaman (Student Member, IEEE) received the B.E. degree in electrical engineering from the National University of Sciences and Technology (NUST), Pakistan, in 2015. He is working towards the Ph.D. degree in quantum information science with the Department of Electronics and Information Convergence Engineering, Kyung Hee University (KHU), South Korea.

Currently, he is a Graduate Research Scholar with the Communications and Quantum Information Laboratory, KHU and an exchange visiting student at Wireless Information and Network Sciences Laboratory, Massachusetts Institute of Technology (MIT). His research interests include quantum control, remote entanglement distribution, and deep reinforcement learning.

Mr. Zaman was the recipient of the Best Paper award at KICS-Fall Conference on Communications in 2019. He served as a reviewer for IEEE JOURNAL ON SELECTED AREAS IN COMMUNICATIONS and several international conferences.

Uman Khalid received his B.S. degree in electronics engineering from the Ghulam Ishaq Khan (GIK) Institute, Topi, Pakistan, in 2015 and his Ph.D. in electronic engineering from Kyung Hee University, South Korea, in February 2023. Since March 2023, he has been a Post-Doctoral Fellow with the Department of Electronic Engineering, Kyung Hee University. His research interests include quantum information science, quantum computing, and quantum metrology.

Hyundong Shin (Fellow, IEEE) received the B.S. degree in Electronics Engineering from Kyung Hee University (KHU), Yongin-si, Korea, in 1999, and the M.S. and Ph.D. degrees in Electrical Engineering from Seoul National University, Seoul, Korea, in 2001 and 2004, respectively.

During his postdoctoral research at the Massachusetts Institute of Technology (MIT) from 2004 to 2006, he was with the Laboratory for Information Decision Systems (LIDS). In 2006, he joined the KHU, where he is currently a Professor in the Department of Electronic Engineering. His research interests include quantum information science, wireless communication, and machine intelligence.

Dr. Shin received the IEEE Communications Society's Guglielmo Marconi Prize Paper Award (2008) and William R. Bennett Prize Paper Award (2012). He served as the Publicity Co-Chair for the IEEE PIMRC (2018) and the Technical Program Co-Chair for the IEEE WCNC (PHY Track 2009) and the IEEE GLOBECOM (Communication Theory Symposium 2012 and Cognitive Radio and Networks Symposium 2016). He was an Editor of IEEE TRANSACTIONS ON WIRELESS COMMUNICATIONS (2007–2012) and IEEE COMMUNICATIONS LETTERS (2013–2015).

Trung Q. Duong (Fellow, IEEE) received his Ph.D. degree in telecommunications systems from Blekinge Institute of Technology, Sweden in 2012. In 2013, he joint Queen's University Belfast, UK, as an academic staff, where he is now a Chair Professor in Telecommunications. He is a Research Chair of the Royal Academy of Engineering. He was a Distinguished Advisory Professor at Inje University, South Korea (2017-2019). He is also a Distinguished Professor at Thuyloi University, Vietnam (2023-2028) and a Distinguished Visiting Professor under Eminent Scholar program at Kyung Hee University, South Korea (2023-2024). His current research interests include quantum communications, wireless communications, signal processing, machine learning, and real-time optimisation.

Dr. Duong has served as an Editor/Guest Editor for the IEEE TRANSACTIONS ON WIRELESS COMMUNICATIONS, IEEE TRANSACTIONS ON COMMUNICATIONS, IEEE TRANSACTIONS ON VEHICULAR TECHNOLOGY, IEEE COMMUNICATIONS LETTERS, IEEE WIRELESS COMMUNICATIONS LETTERS, IEEE WIRELESS COMMUNICATIONS, IEEE COMMUNICATIONS MAGAZINES, and IEEE JOURNAL ON SELECTED AREAS IN COMMUNICATIONS. Currently, he is serving as an Executive Editor for IEEE COMMUNICATIONS LETTERS. He received the Best Paper Award at the IEEE VTC-Spring 2013, IEEE ICC 2014, IEEE GLOBECOM 2016, 2019, 2022, IEEE DSP 2017, and IWCMC 2019. He is the recipient of prestigious Royal Academy of Engineering Research Fellowship (2015-2020) and has won a prestigious Newton Prize in 2017. He is a Fellow of Asia-Pacific Artificial Intelligence Association (AAIA).

Moe Z. Win (Fellow, IEEE) is a Professor at the Massachusetts Institute of Technology (MIT) and the founding director of the Wireless Information and Network Sciences Laboratory. Prior to joining MIT, he was with AT&T Research Laboratories and with NASA Jet Propulsion Laboratory.

His research encompasses fundamental theories, algorithm design, and network experimentation for a broad range of real-world problems. His current research topics include ultra-wideband systems, network localization and navigation, network interference exploitation, and quantum information science. He has served the IEEE Communications Society as an elected Member-at-Large on the Board of Governors, as elected Chair of the Radio Communications Committee, and as an IEEE Distinguished Lecturer. Over the last two decades, he held various editorial positions for IEEE journals and organized numerous international conferences. Recently, he has served on the SIAM Diversity Advisory Committee.

Dr. Win is an elected Fellow of the AAAS, the EURASIP, the IEEE, and the IET. He was honored with two IEEE Technical Field Awards: the IEEE Kiyo Tomiyasu Award (2011) and the IEEE Eric E. Sumner Award (2006, jointly with R. A. Scholtz). His publications, co-authored with students and colleagues, have received several awards. Other recognitions include the MIT Everett Moore Baker Award (2022), the IEEE Vehicular Technology Society James Evans Avant Garde Award (2022), the IEEE Communications Society Edwin H. Armstrong Achievement Award (2016), the Cristoforo Colombo International Prize for Communications (2013), the Copernicus Fellowship (2011) and the *Laurea Honoris Causa* (2008) from the Università degli Studi di Ferrara, and the U.S. Presidential Early Career Award for Scientists and Engineers (2004). He is an ISI Highly Cited Researcher.